Table S1 Definitions, values and units of parameters in MIMICS.

Parameter	Description	Value	Unit
Carbon pools			
LIT_m	Metabolic litter pool	-	mg C cm^{-3}
LIT_S	Structural litter pool	-	mg C cm^{-3}
MIC_r	Microorganism with copiotrophic growth strategy	-	mg C cm^{-3}
MIC_k	Microorganism with oligotrophic growth strategy	-	mg C cm^{-3}
SOC_p	Physically-protected SOC pool	-	mg C cm^{-3}
SOC_c	Chemical protected SOC pool	-	mg C cm^{-3}
SOC_a	Available SOC pool	-	mg C cm^{-3}
Litter input parameters			
f_{met}	Partitioning of litter inputs to LIT_m	0.85-0.013 (lignin/N)	-
$f_{i,met}$	Fraction of litter inputs transferred to SOC_p	0.05	-
$f_{i,stru}$	Fraction of litter inputs transferred to SOC_c	0.05	-
Microbial decomposition parameters			
V_{max}	Microbial maximum reaction velocity	-	mg C (mg MIC)$^{-1}$ h^{-1}
K_m	Half-saturation constant	-	mg C cm^{-3}
V_{slope}	Regression coefficient (Eq. 2)	0.063 [a]	ln (mg C (mg MIC)$^{-1}$ h^{-1}) °C^{-1}
V_{int}	Regression intercept (Eq. 2)	5.47 [a]	ln (mg C (mg MIC)$^{-1}$ h^{-1})
av	Tuning coefficient (Eq. 2)	8×10^{-6} [a]	-
V_{mod-r}	Modifies V_{max} for fluxes into MIC_r	10, 2, 10 [b]	-
V_{mod-k}	Modifies V_{max} for fluxes into MIC_k	3,3,2 [c]	-
K_{slope}	Regression coefficient (Eq. 3)	0.017, 0.027, 0.017 [b, c]	ln (mg C cm^{-3}) °C^{-1}
K_{int}	Regression intercept (Eq. 3)	3.19 [a]	ln (mg C cm^{-3})
ak	Tuning coefficient (Eq. 3)	10 [a]	-
K_{mod-r}	Modifies K_m for fluxes into MIC_r	0.125,0.5,0.25 $\times P_{scalar}$ [b]	-
K_{mod-k}	Modifies K_m for fluxes into MIC_k	0.5,0.25,0.167 $\times P_{scalar}$ [c]	-
P_{scalar}	Physical protection scalar used in K_{mod}	$(2.0 \times (2.0 \times e^{-2\sqrt{fclay}})^{-1}$	-
MGE	Microbial growth efficiency	0.5,0.25,0.7,0.35 [d]	mg mg^{-1}
k_{mic}	Microbial biomass turnover rate	$5.2 \times 10^{-4} \times e^{0.3(fmet)} \times \tau_{mod}$ [e]	h^{-1}
		$2.4 \times 10^{-4} \times e^{0.1(fmet)} \times \tau_{mod}$ [e]	
τ_{mod}	Modifies microbial turnover rate	$0.8 < \sqrt{NPP/100} < 1.2$	-
a_τ	Tuning coefficient of K_{mic}	1.0	-
f_{rp}	Fraction of K_{mic} of MIC_r partitioned to SOC_p	$min(1.0, 0.13 \times e^{1.3(fclay)})$ [f]	-
f_{kp}	Fraction of K_{mic} of MIC_k partitioned to SOC_p	$min(1.0, 0.02 \times e^{0.8(fclay)})$ [f]	
f_{rc}	Fraction of K_{mic} of MIC_r partitioned to SOC_c	$min(1.0 - f_{rp}, 1.06 \times e^{-2.6(fmet)})$ [f]	-
f_{kc}	Fraction of K_{mic} of MIC_k partitioned to SOC_c	$min(1.0 - f_{kp}, 8.93 \times e^{-2.6(fmet)})$ [f]	
f_{ra}	Fraction of K_{mic} of MIC_r partitioned to SOC_a	$1.0 - f_{rp} - f_{rc}$	-
f_{ka}	Fraction of K_{mic} of MIC_k partitioned to SOC_a	$1.0 - f_{kp} - f_{kc}$	
β	Density-dependence exponent in Eq. 6	-	-
Protected carbon parameters			
D	Deprotection rate from SOM_p to SOM_a	Eq. 5	h^{-1}
KO	Further modifies K_m for oxidation of SOM_c	4, 4 [e]	-
k_d	Tuning coefficient of the deprotection rate	-	-
K_{ads}	The sorption rate of SOC_p in Eq. 8	Eq. 8	h^{-1}
k_{ba}	The binding affinity in Eq. 8	1~16 [g]	(mg C mg^{-3})$^{-1}$
Q_{max}	The maximum sorption capacity of SOC_p	Eq. 9	mg C cm^{-3}

Parameter	Description	Value	Unit
Biochar-related parameters			
f_{bp}	Fraction of biochar carbon partitioned into SOC_p	0.6	-
f_{ba}	Fraction of biochar carbon partitioned into SOC_a	0.03-0.3 [h]	-
f_{bc}	Fraction of biochar carbon partitioned into SOC_c	$1.0 - f_{bp} - f_{ba}$	-
f_{loss}	Biochar fraction loss during addition		
f_d	Coefficients for adjusting the deprotection rate of SOC_p with biochar addition in Eq. 15	-0.15 ~0.15 [h]	ha t^{-1} C
f_v	Coefficients for adjusting the microbial decomposition velocity with biochar addition in Eq. 16	-0.15 ~0.15 [h]	ha t^{-1} C

[a] From observations in German et al. (2012), as used in Wieder et al. (2014, 2015).

[b] For LIT_m, LIT_s, and SOC_a, fluxes entering MIC_r, respectively.

[c] For LIT_m, LIT_s, and SOC_a, fluxes entering MIC_k, respectively.

[d] 0.5 is the MGE of C fluxes from LIT_m and SOC_a to MIC_r, 0.25 is for C flux from LIT_s to MIC_r, 0.7 is for fluxes from LIT_s and SOC_a to MIC_k, 0.35 is for C flux from LIT_m to MIC_k.

[e] For MIC_r and MIC_k, respectively.

[f] Values from Zhang et al. (2020).

[g] Values from Wang et al. (2020).

[h] Ranges from Archontoulis et al. (2016).

Table S2 The modifications for various MIMICS versions.

	Model	**Description**
MIMICS	MIMICS-def	The default model version with modified parameters related to crop properties (Section 2.2.5).
	MIMICS-T	Considering the density-dependent microbial turnover rate (denoted as "T", Eq. 6).
	MIMICS-TS	Adding the sorption process of SOC_p based on MIMICS-T ("S", Eq. 7-9).
	MIMICS-TSM_a	Including soil moisture effects from CENTURY model ("M_a") based on MIMICS-TS.
	MIMICS-TSM_b	Including soil moisture effects from ORCHIDEE-SOM model ("M_b") based on MIMICS-TS.
	MIMICS-TSM_c	Including soil moisture effects from Yan et al. (2018) ("M_c") based on MIMICS-TS.
MIMICS-BC	MIMICS-TSM_b	Including both the sorption process and soil moisture effects but without biochar related parameters for biochar addition.
	MIMICS-BC_D	Including biochar effects on SOC by modifying deprotection rate of SOC_p in the MIMICS-TSM_b (Eq. 15).
	MIMICS-BC_{DV}	Including further biochar effects on SOC by modifying the microbial maximum reaction velocity in MIMICS-TSM_b (Eq. 16).

Table S3 Definitions and values of modified parameters used in default MIMICS.

Parameters[d]	Description	Original values[a]	Modified values
cn_leaf	The ratio of carbon to nitrogen in leaf	30	25[b]
cn_root	The ratio of carbon to nitrogen in root	75	45[b]
cn_wood	The ratio of carbon to nitrogen in wood	200	50[b]
lig_c_leaf	The ratio of lignin to carbon in leaf	0.1	0.12[b]
lig_c_root	The ratio of lignin to carbon in root	0.1	0.40[b]
lig_c_wood	The ratio of lignin to carbon in wood	0.15	0.15[b]
HI	Harvest index	-	0.45[c]

[a] Values based on Zhang et al. (2020).

[b] Estimated values from Abiven et al. (2005).

[c] From value in Hicke & Lobell (2004).

[d] These parameters were assumed unchanged with biochar addition.

Table S4 Prior parameter values, optimized values and ranges in the parameter optimization for various MIMICS versions.

Datasets	Model	Parameter	Prior value	Optimized value	Range[c]	Units
MIMICS (58 sites)	MIMICS-def	a_v	10	13.05	[0,30]	-
		a_k	5	11.70	[0,20]	-
		k_d	0.5	0.94	[0,3]	-
	MIMICS-T	a_v	10	8.97	[0,30]	-
		a_k	5	16.43	[0,20]	-
		k_d	0.5	1.82	[0,3]	-
		β	1	1.66	[0,2]	-
	MIMICS-TS	a_v	10	16.92	[0,30]	-
		a_k	5	12.52	[0,20]	-
		k_d	0.5	1.65	[0,3]	-
		β	1	1.41	[0,2]	-
		k_{ba}	6	5.07	[1,16]	-
		c_1	0.3	0.52	[0,0.8]	-
		c_2	3.0	3.7	[0,5]	-
	MIMICS-TSM_a	a_v	10	11.75	[0,30]	-
		a_k	5	10.07	[0,20]	-
		k_d	0.5	1.39	[0,3]	-
		β	1	1.50	[0,2]	-
		k_{ba}	6	5.17	[1,16]	-
		c_1	0.3	0.42	[0,0.8]	-
		c_2	3	3.48	[0,5]	-
	MIMICS-TSM_b	a_v	10	15.91	[0,30]	-
		a_k	5	13.10	[0,20]	-
		k_d	0.5	1.60	[0,3]	-
		β	1	1.47	[0,2]	-
		k_{ba}	6	2.95	[1,16]	-
		c_1	0.3	0.51	[0,0.8]	-
		c_2	3	3.86	[0,5]	-
	MIMICS-TSM_c	a_v	10	17.50	[0,30]	-
		a_k	5	13.33	[0,20]	-
		k_d	0.5	1.13	[0,3]	-
		β	1	1.41	[0,2]	-
		k_{ba}	6	4.17	[1,16]	-
		c_1	0.3	0.42	[0,0.8]	-
		c_2	3	3.65	[0,5]	-
MIMICS-BC (134 sites)	MIMICS-TSM_b	none	none	none	none	none
	MIMICS-BC_D	f_d	-0.002	-0.0038[a] (-0.0131[b])	[-0.15,0.15]	ha t^{-1} C
	MIMICS-BC_{DV}	f_d	-0.002	-0.0083[a] (-0.0095[b])	[-0.15,0.15]	ha t^{-1} C
		f_v	0.05	0.008[a] (-0.0097[b])	[-0.15,0.15]	ha t^{-1} C

[a] The optimized parameter values using the short-term SOC data.

[b] The optimized parameter values using the long-term (extended to 8 yr) SOC data.

[c] The prescribed parameter ranges of a_v, a_k, k_d, β are from Zhang et al. (2020). k_{ba} is from Wang et al. (2020). c_1 and c_2 are estimated from Mayes et al. (2012). f_d and f_v are from Archontoulis et al. (2016).

Table S5 The MIMICS model performance with cross-validation.

Dataset	Model	**Train 80% (46 sites)**			**Test 20% (12 sites)**		
		R^2	RMSE (g kg^{-1})	AIC	R^2	RMSE (g kg^{-1})	AIC
This study (total 58 sites)	MIMICS-def	0.39	4.96	153.33	0.34	5.06	44.76
	MIMICS-T	0.49	4.55	147.21	0.33	5.04	46.36
	MIMICS-TS	0.52	4.42	150.76	0.38	4.96	52.14
	MIMICS-TSM_b	0.50	4.54	153.04	0.33	5.03	52.63

Notes: RMSE is the root mean square error, AIC is the Akaike information criterion.

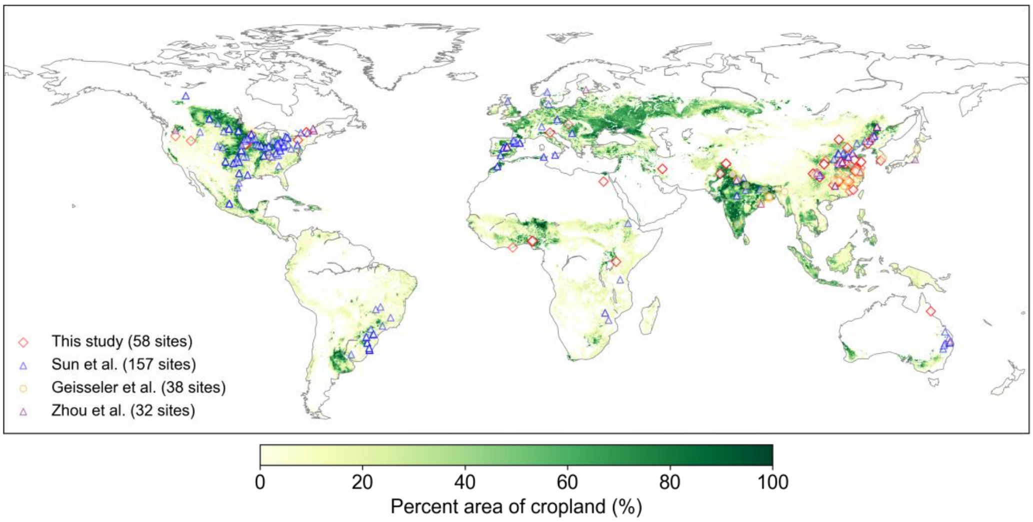

Fig. S1 Locations of field cropland SOC measurements with or without biochar addition collected in this study and SOC measurements without biochar addition from Sun et al, (2020), Geisseier et al., (2017) and Zhou et al., (2017). Number of sites is also shown in the legend. Note that one site may have multiple paired SOC data due to various experimental conditions of biochar addition in our collected 58 sites. The cropland area percentage in each 10 km × 10 km grid cell is derived from EarthStat (http://www.earthstat.org; Ramankutty et al., 2008).

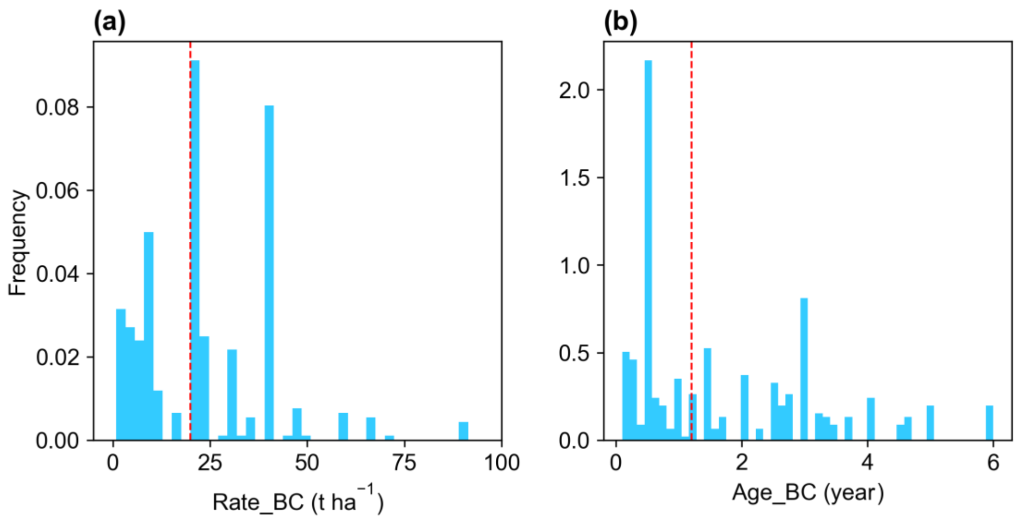

Fig. S2 The frequency distribution of (a) biochar application rates (Rate_BC) and (b) biochar addition periods (Age_BC). Red dotted lines indicate the median values.

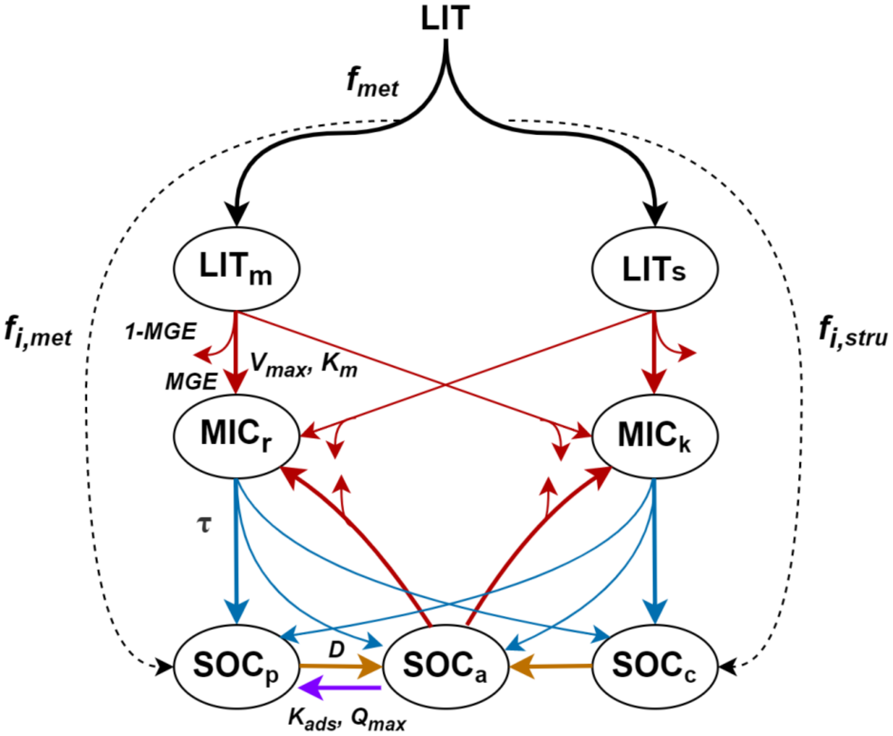

Fig. S3 Framework of the MIMICS model (adapted from Wieder et al., 2015). The litter inputs (LIT) are divided into metabolic (LIT_m) and structural litter pools (LIT_s) according to the litter quality (f_{met}, i.e., fraction of litter to LIT_m). Microbial growth efficiency (MGE) determines the carbon fluxes from the two litter pools and the available SOC pool (SOC_a) into microbial biomass pools and heterotrophic respiration. The turnover of microbial biomass (τ) depends on the microbial functional types (MIC_r and MIC_k for r- and k-strategy). The three SOC pools represent the available, physically protected, and chemically recalcitrant SOC (SOC_a, SOC_p, and SOC_c, respectively). SOC in the protected pools (i.e., SOC_p and SOC_c) are released to the available SOC pool (SOC_a) over time (yellow arrow lines). The new added adsorption process associated with adsorption rate (K_{ads}) and the maximum sorption capacity (Q_{max}) from SOC_a to SOC_p are presented as the purple arrow lines. Detailed description of model parameters and carbon fluxes can be found in Table S1 and Wieder et al. (2015).

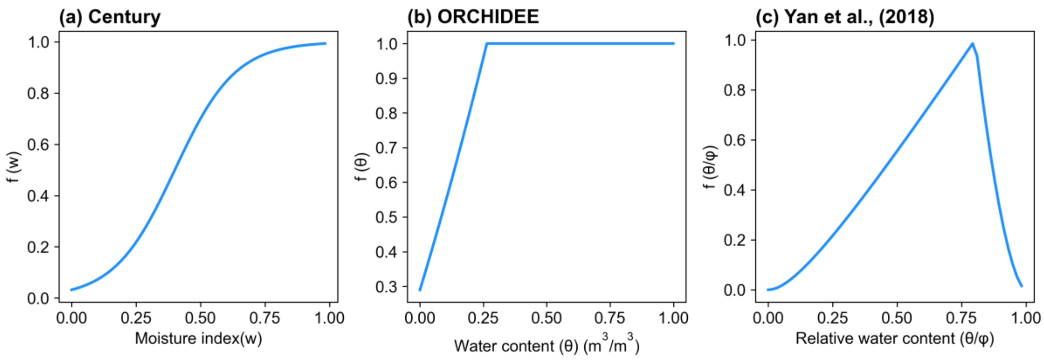

Fig. S4 Soil moisture functions from (a) the Century model (Parton et al., 2000), (b) the ORCHIDEE-SOM model (Camino-Serrano et al., 2018) and (c) the mechanism-based soil moisture function from Yan et al. (2018). *w* is soil moisture indicator (AI, i.e., precipitation/potential evapotranspiration). θ is soil water content, φ is soil porosity, and θ/φ is relative water content.

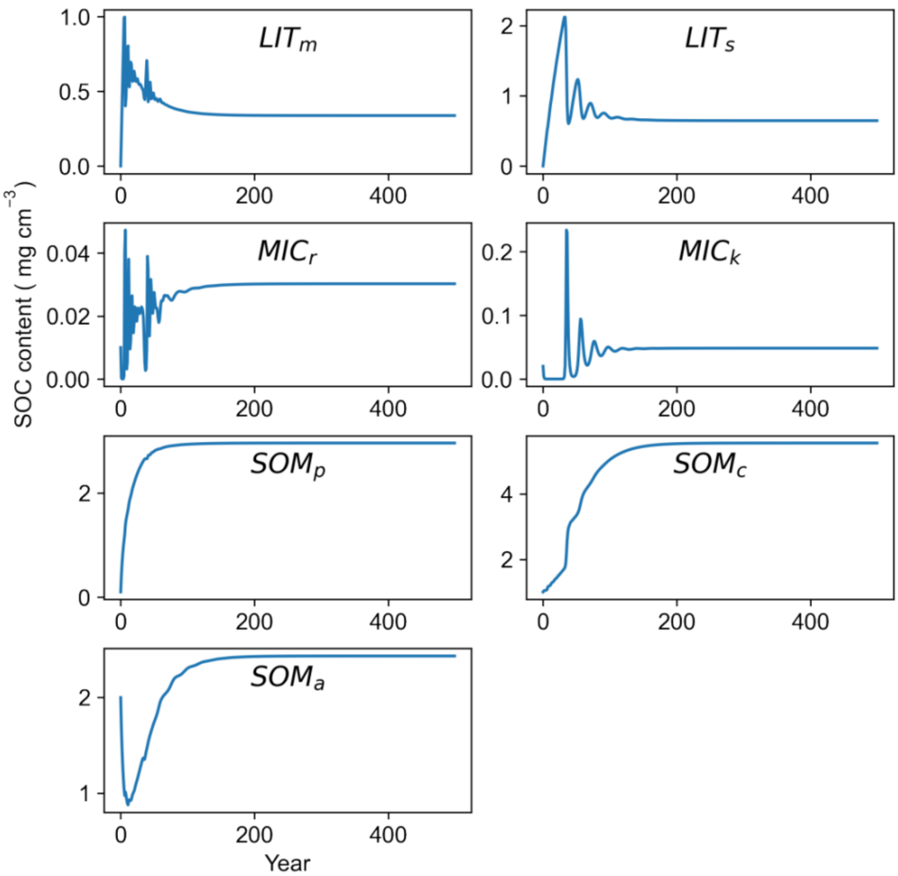

Fig. S5 Temporal changes of seven SOC pools from a simulation of the MIMICS-TSM$_b$ version for 500 years using one random site (Lat, Lon =28.1 °N, 113.2 °E) as an example.

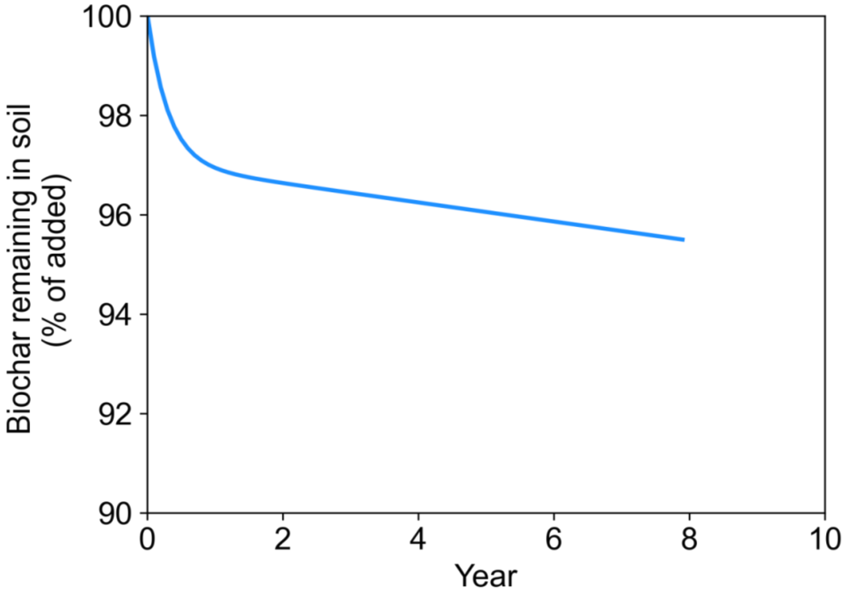

Fig. S6 The biochar decomposition curve fitted with experimental data from Wang et al. (2016) using a double first-order exponential decay model ($BC_{remain\%} = 3.02 \times e^{(-3.24 \times age\_bc)} + 97.02 \times e^{(-0.002 \times age\_bc)}$).

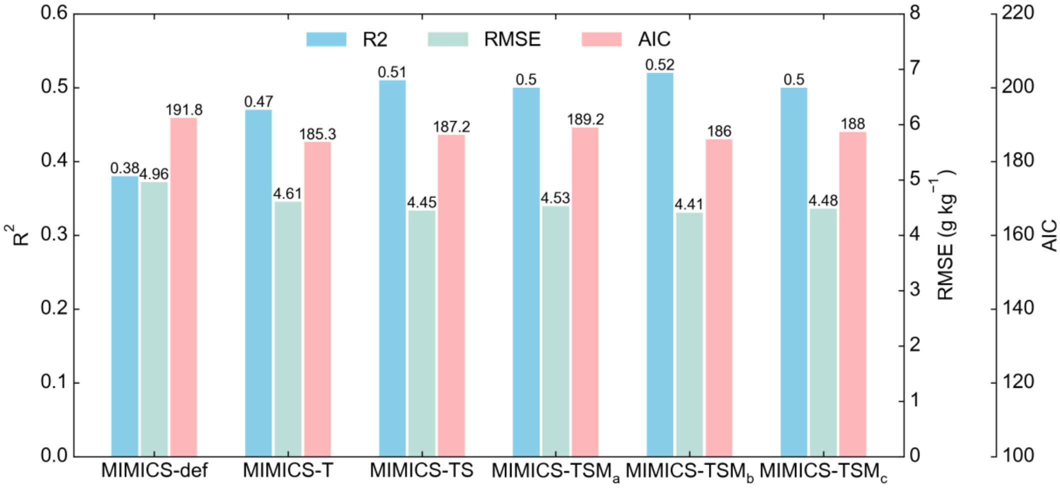

Fig. S7 Comparison of R^2, RMSE and AIC of all MIMICS versions.

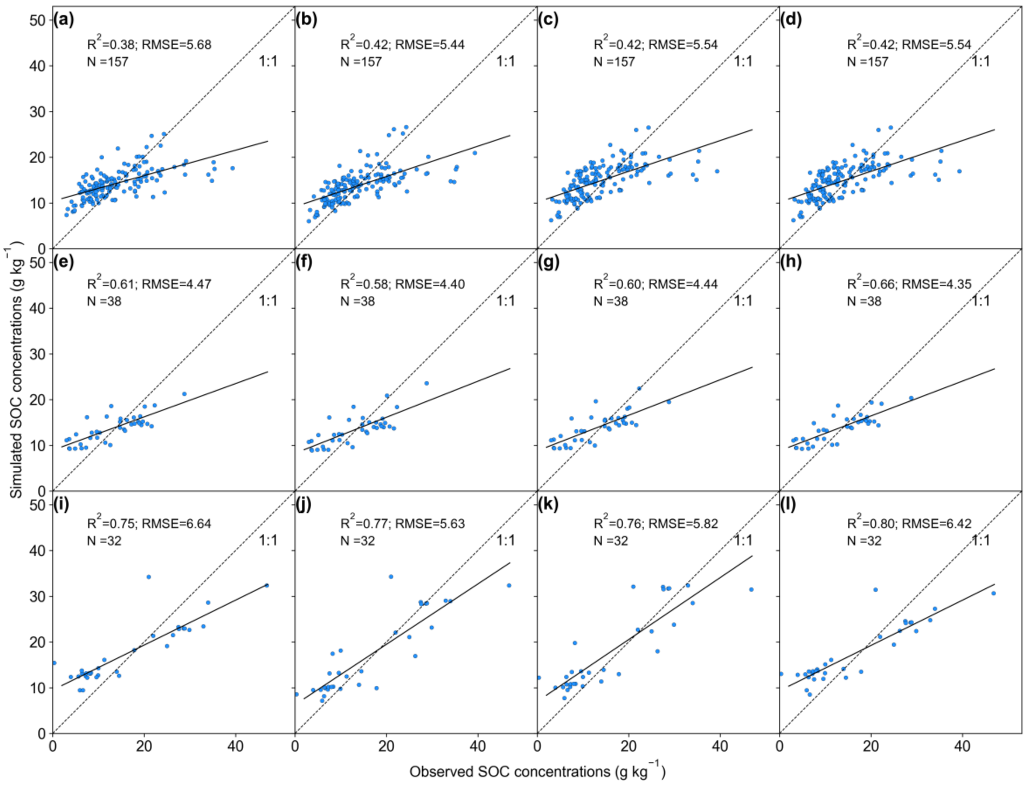

Fig. S8 Relationship between observed and simulated SOC concentrations by MIMICS-def (a, e, i), MIMICS-T (b, f, j), MIMICS-TS (c, g, k) and MIMICS-TSM$_b$ (d, h, l). The observed SOC concentrations are from (a-d) Sun et al. (2020), (e-h) Geisseler et al. (2017), (i-l) Zhou et al. (2017). The unit of RMSE is g kg^{-1}.

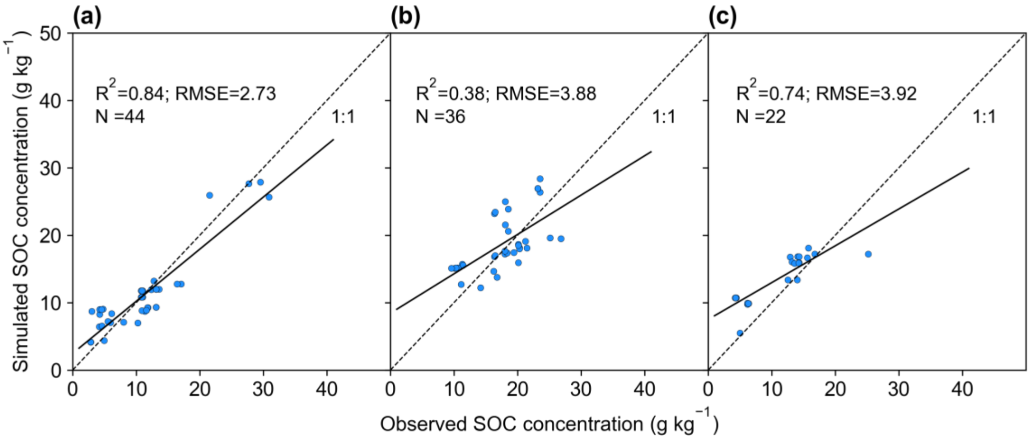

Fig. S9 Relationship between observed and simulated SOC concentrations by MIMICS-TSM$_b$ for (a) maize, (b) rice and (c) wheat. The unit of RMSE is g kg^{-1}.

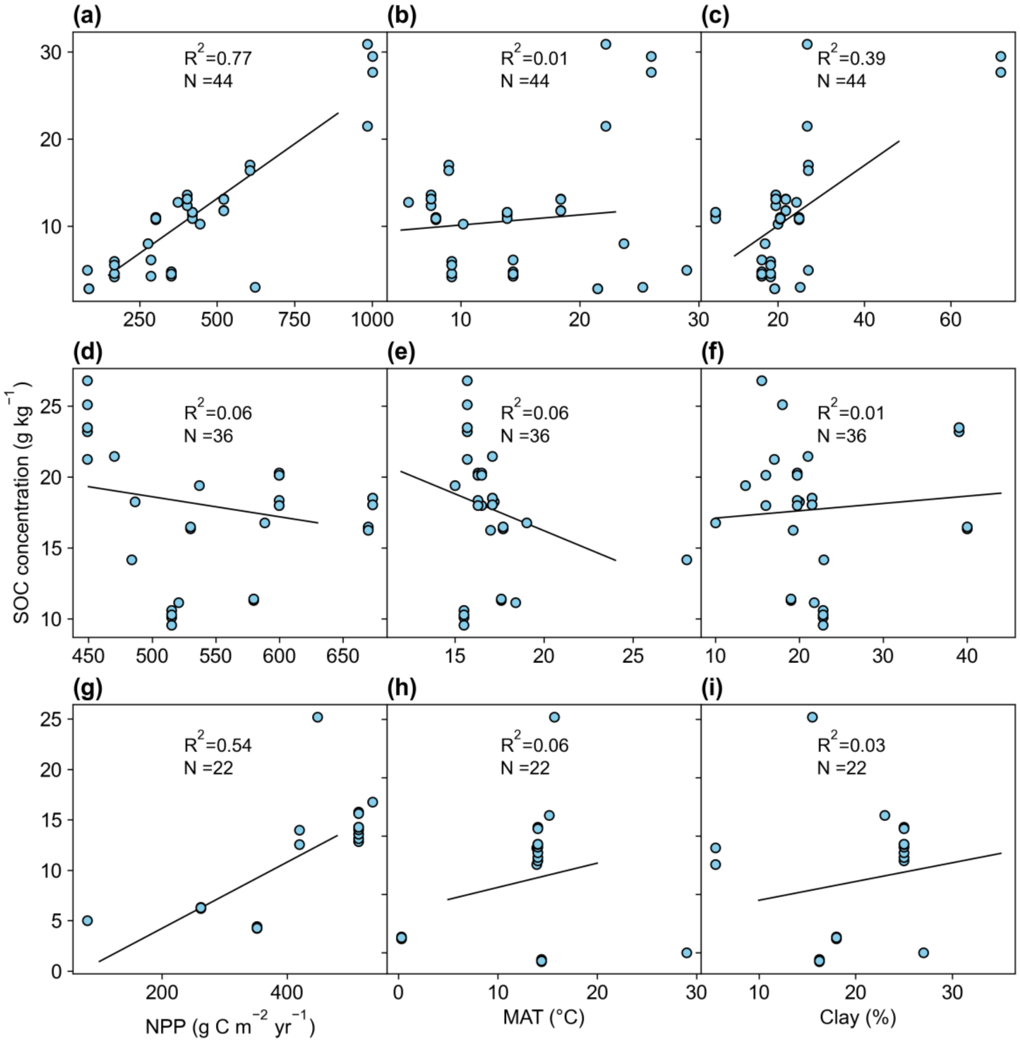

Fig. S10 Correlation between SOC concentrations with NPP, MAT and Clay for maize (a-c), rice (d-f) and wheat (g-i).

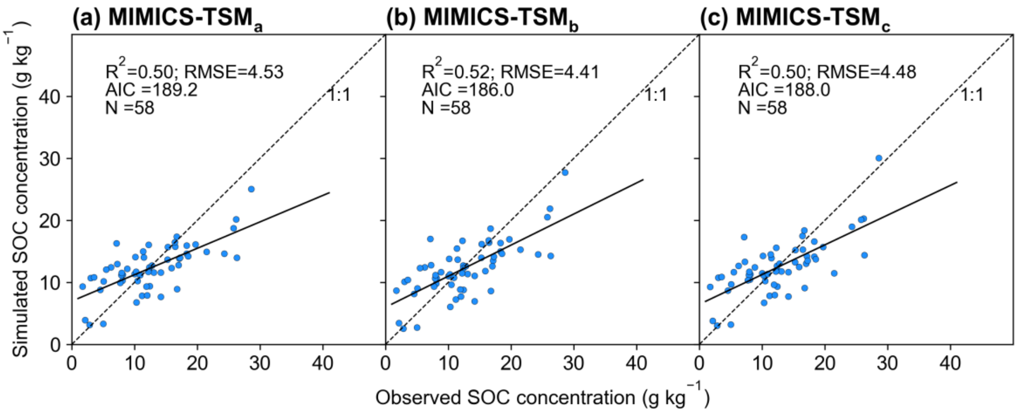

Fig. S11 Relationships between observed and simulated SOC concentrations by (a) MIMICS-TSM$_a$, (b) MIMICS-TSM$_b$ and (c) MIMICS-TSM$_c$, respectively.

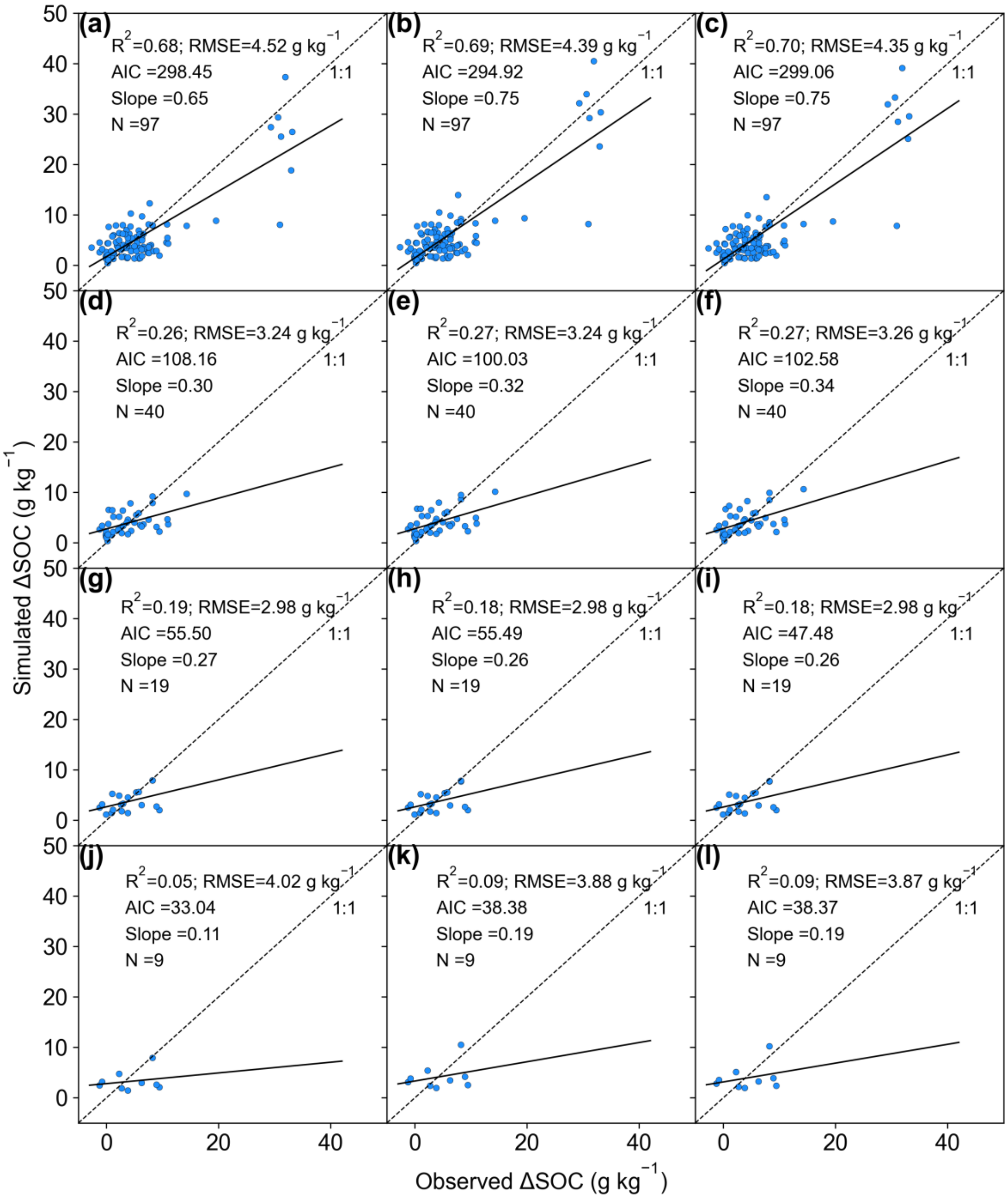

Fig. S12 Relationship between observed and simulated SOC changes (ΔSOC) for data with Age_BC ≥ 3yr (a-c), Age_BC ≥ 4yr (d-f), Age_BC ≥ 5yr (g-i) and Age_BC ≥ 6yr (j-l) using three MIMICS versions: MIMICS-TSM_b (a, d, g, j), MIMICS-BC_D (b, e h, k) and MIMICS-BC_{DV} (c, f, i, l).

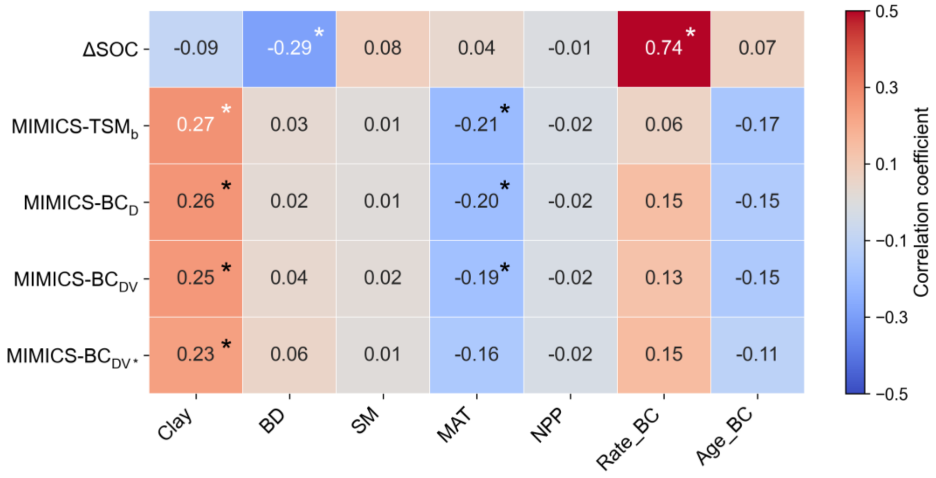

Fig. S13 Correlations between the observed short-term SOC changes after biochar addition (ΔSOC) and soil- (Clay, BD, SM), climate- (MAT), biological- (NPP) and biochar-related (Rate_BC, Age_BC) variables in first row. The other rows are for the ΔSOC biases in short-term between observations and simulations by MIMICS-TSM$_b$, MIMICS-BC$_D$, MIMICS-BC$_{DV}$ and MIMICS-BC$_{DV*}$. MIMICS-BC$_{DV*}$ is the version with four parameters optimized (i.e., f_d, f_v, f_{bp}, f_{ba}). Asterisk indicates significant correlations ($p < 0.05$).

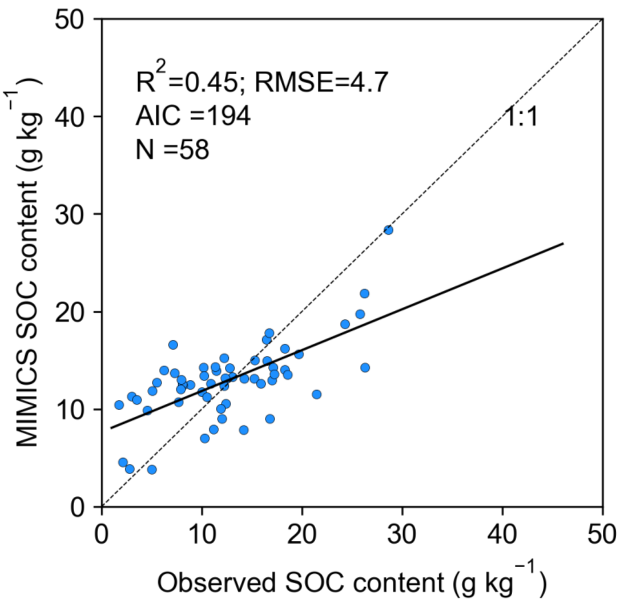

Fig. S14 Relationships between observed and simulated SOC concentrations by MIMICS-TSM_b assuming that the soil moist factor ($f_{m2}(\theta)$, Eq. 11) were multiplied by V_{max} and microbial turnover (τ) of MIC_r and MIC_k , instead of by V_{max} and K_m in **Section 2.2.4**.

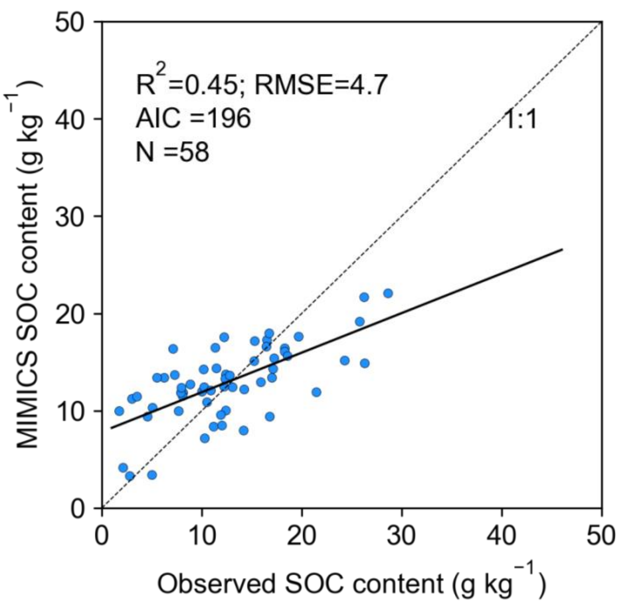

Fig. S15 Relationships between observed and simulated SOC concentrations by MIMICS-TSM_b with NPP optimized additionally (i.e., total 8 parameters: a_v, a_k, k_d, β, k_{ba}, c_1, c_2, f_{npp}).

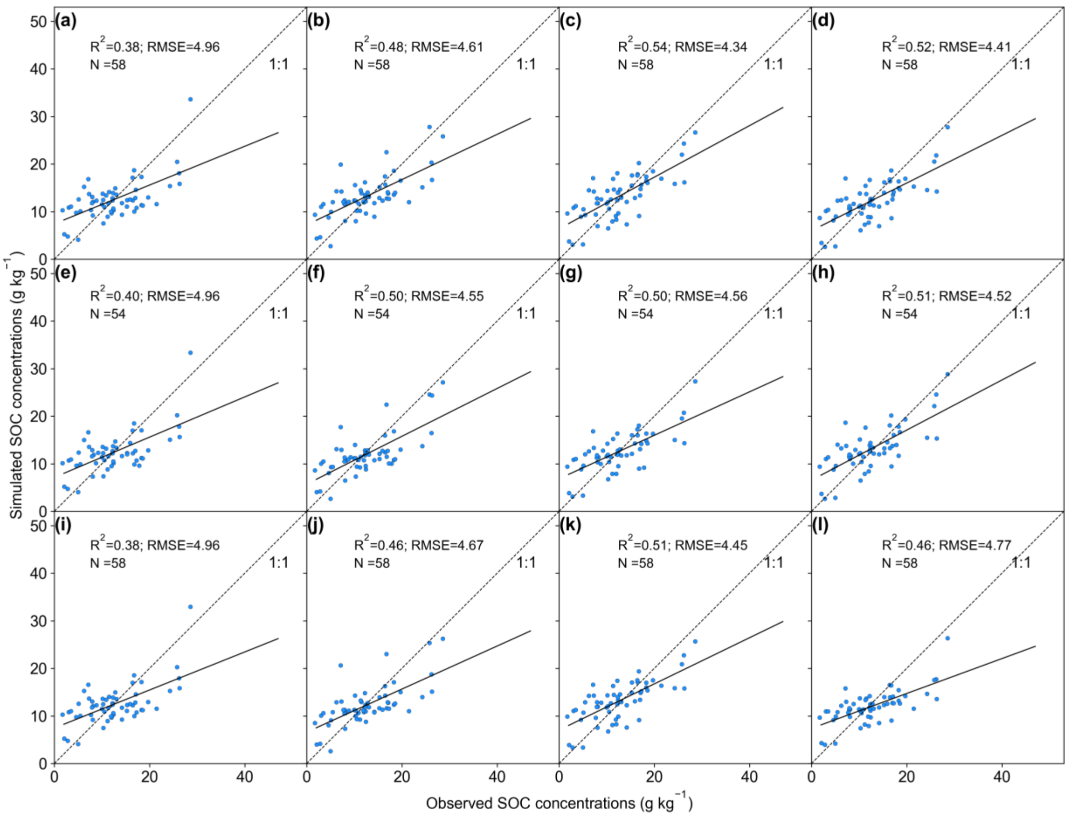

Fig. S16 Relationships between observed and simulated SOC concentrations by MIMICS-def (a, e, i), MIMICS-T (b, f, j), MIMICS-TS (c, g, k) and MIMICS-TSM$_b$ (d, h, l). The MIMICS versions in the first row (a-d) used the reverse Michaelis-Menten kinetics in SOC decomposition processes. The MIMICS versions in the second row were validated against SOC concentrations aggregated within each 0.5 °grid cell. The MIMICS versions in the last row consider the tillage effects on SOC by assuming a 30% increase in the deprotection rate of SOC$_p$. The unit of RMSE is g kg^{-1}.

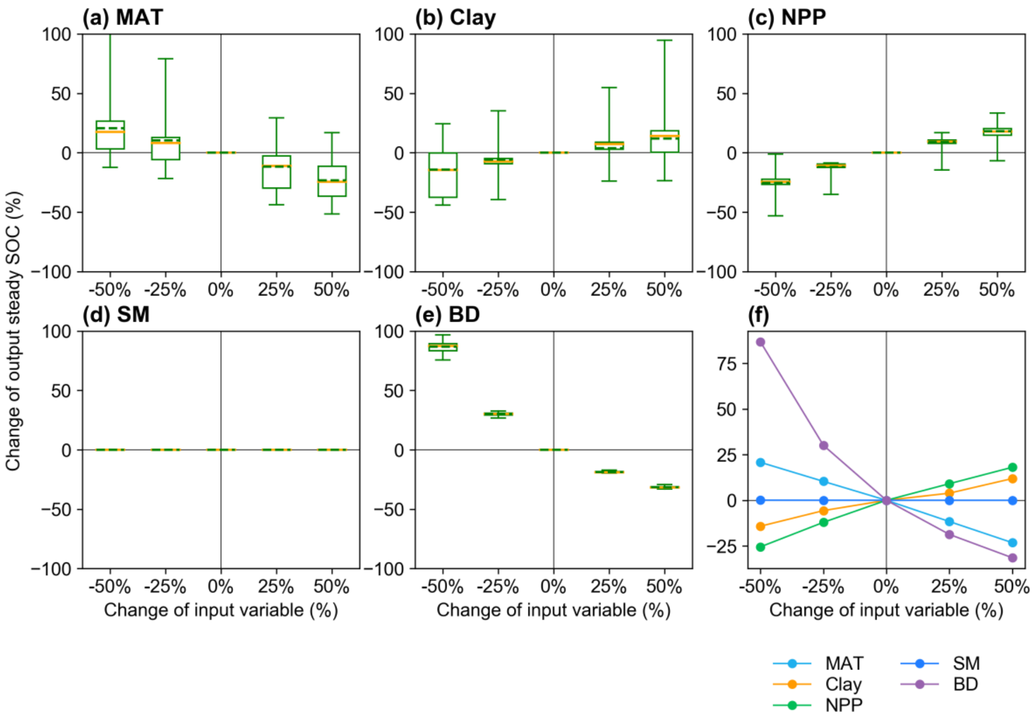

Fig. S17 Sensitivity analysis of responses of the steady SOC simulated by MIMICS to input variables of (a) MAT, (b) Clay, (c) NPP, (d) SM and (e) BD with different perturbation levels. The yellow line and green dotted line in the boxplot are median and mean values of the output steady SOC changes in 58 sites. The average SOC changes in all sites for the four perturbation levels are shown in (f).

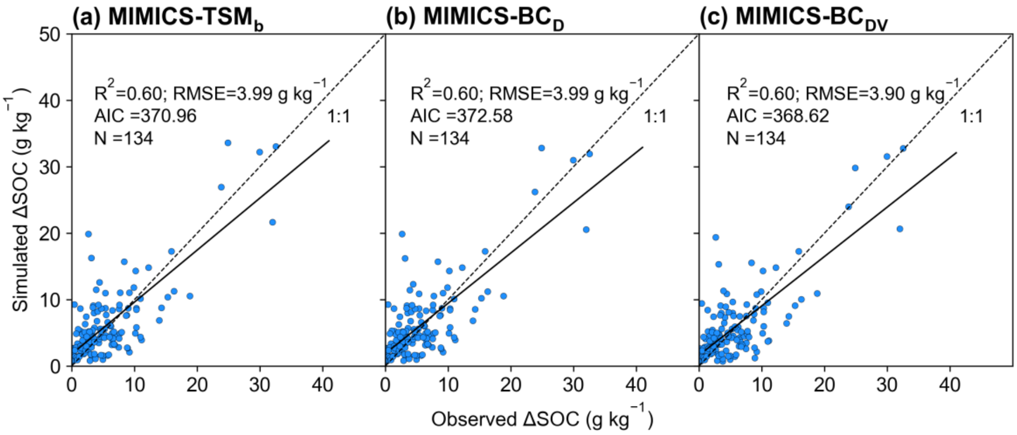

Fig. S18 Relationships of short-term SOC changes after biochar addition between observations and models with (a) MIMICS-TSM$_b$, (b) MIMICS-BC$_D$ and (c) MIMICS-BC$_{DV}$. (f_{ba}=2%)

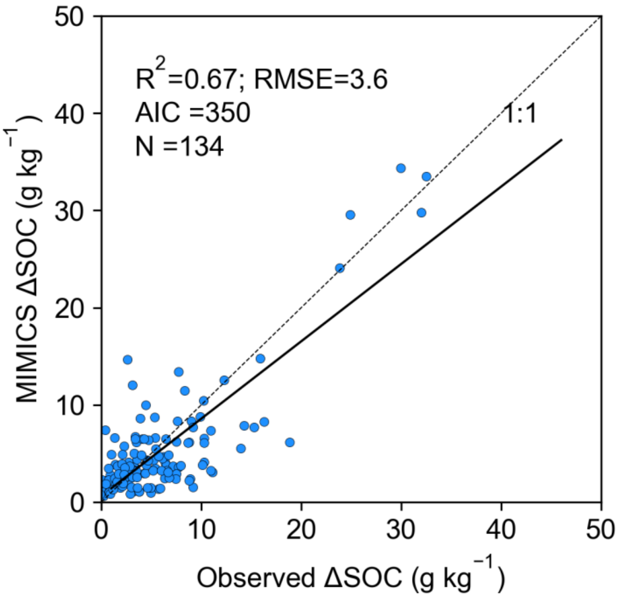

Fig. S19 Relationships of short-term SOC changes after biochar addition between observations and models simulated with MIMICS-BC version with four parameters optimized (f_d=-0.0135, f_v=0.0196, f_{bp}=0.5957 and f_{ba}=0.2906). The unit of RMSE is g kg^{-1}.

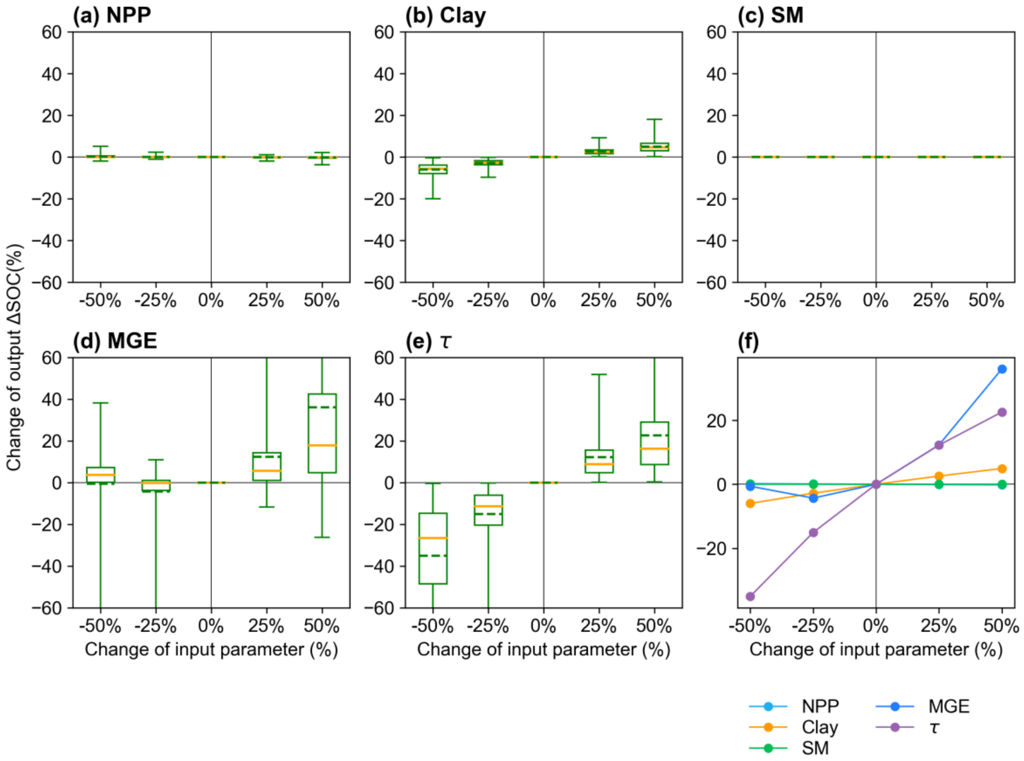

Fig. S20 Sensitivity analysis of MIMICS-BC model input variables of (a) NPP, (b) Clay, (c) SM and parameters of (d) *MGE* (microbial growth efficiency, Fig. S3) and (e) τ (microbial biomass turnover, Fig. S3). The yellow line and green dotted line in boxplot are median and mean values of output variable change (i.e., change of ΔSOC, Eq. 19). The means of ΔSOC changes with perturbations in all sites are plot in (f).

References

Abiven, S., Recous, S., Reyes, V., & Oliver, R.: Mineralisation of C and N from root, stem and leaf residues in soil and role of their biochemical quality, *Biology and Fertility of Soils, 42*, 119-128, doi:10.1007/s00374-005-0006-0, 2005.

Archontoulis, S. V., Huber, I., Miguez, F. E., Thorburn, P. J., Rogovska, N., & Laird, D. A.: A model for mechanistic and system assessments of biochar effects on soils and crops and trade-offs, *GCB Bioenergy, 8*, 1028-1045, doi:10.1111/gcbb.12314, 2016.

Camino-Serrano, M., Guenet, B., Luyssaert, S., Ciais, P., Bastrikov, V., De Vos, B., Gielen, B., Gleixner, G., Jornet-Puig, A., Kaiser, K., Kothawala, D., Lauerwald, R., Peñuelas, J., Schrumpf, M., Vicca, S., Vuichard, N., Walmsley, D., & Janssens, I. A.: ORCHIDEE-SOM: modeling soil organic carbon (SOC) and dissolved organic carbon (DOC) dynamics along vertical soil profiles in Europe, *Geoscientific Model Development, 11*, 937-957, doi:10.5194/gmd-11-937-2018, 2018.

Geisseler, D., Linquist, B. A., & Lazicki, P. A.: Effect of fertilization on soil microorganisms in paddy rice systems – A meta-analysis, *Soil Biology and Biochemistry, 115*, 452-460, doi:10.1016/j.soilbio.2017.09.018, 2017.

German, D. P., Marcelo, K. R., Stone, M. M., & Allison, S. D.: The M ichaelis–M enten kinetics of soil extracellular enzymes in response to temperature: a cross-latitudinal study, *Global Change Biology, 18*, 1468-1479. 2012.

Hicke, J. A., & Lobell, D. B.: Spatiotemporal patterns of cropland area and net primary production in the central United States estimated from USDA agricultural information, *Geophysical Research Letters, 31*. 2004.

Mayes, M. A., Heal, K. R., Brandt, C. C., Phillips, J. R., & Jardine, P. M.: Relation between Soil Order and Sorption of Dissolved Organic Carbon in Temperate Subsoils, *Soil Science Society of America Journal, 76*, 1027-1037, doi:10.2136/sssaj2011.0340, 2012.

Parton, W. J., Morgan, J. A., Kelly, R. H., & Ojima, D.: Modeling soil C responses to environmental change in grassland systems[M] The potential of US grazing lands to sequester carbon and mitigate the greenhouse effect. 2000.

Ramankutty, N., Evan, A. T., Monfreda, C., & Foley, J. A.: Farming the planet: 1. Geographic distribution of global agricultural lands in the year 2000, *Global Biogeochemical Cycles, 22*, doi:10.1029/2007gb002952, 2008.

Sun, W., Canadell, J. G., Yu, L., Yu, L., Zhang, W., Smith, P., Fischer, T., & Huang, Y.: Climate drives global soil carbon sequestration and crop yield changes under conservation agriculture, *Glob Chang Biol, 26*, 3325-3335, doi:10.1111/gcb.15001, 2020.

Wang, G., Huang, W., Zhou, G., Mayes, M. A., & Zhou, J.: Modeling the processes of soil moisture in regulating microbial and carbon-nitrogen cycling, *Journal of Hydrology, 585*, doi:10.1016/j.jhydrol.2020.124777, 2020.

Wang, J., Xiong, Z., & Kuzyakov, Y.: Biochar stability in soil: meta-analysis of decomposition and priming effects, *Global Change Biology Bioenergy, 8*, 512-523, doi:10.1111/gcbb.12266, 2016.

Wieder, W. R., Grandy, A. S., Kallenbach, C. M., & Bonan, G. B.: Integrating microbial physiology and physio-chemical principles in soils with the MIcrobial-MIneral Carbon Stabilization (MIMICS) model, *Biogeosciences, 11*, 3899-3917, doi:10.5194/bg-11-3899-2014, 2014.

Wieder, W. R., Grandy, A. S., Kallenbach, C. M., Taylor, P. G., & Bonan, G. B.: Representing life in the Earth system with soil microbial functional traits in the MIMICS model, *Geoscientific Model Development, 8*, 1789-1808, doi:10.5194/gmd-8-1789-2015, 2015.

Yan, Z., Bond-Lamberty, B., Todd-Brown, K. E., Bailey, V. L., Li, S., Liu, C., & Liu, C.: A moisture function of soil heterotrophic respiration that incorporates microscale processes, *Nat Commun, 9*, 2562, doi:10.1038/s41467-018-04971-6, 2018.

Zhang, H., Goll, D. S., Wang, Y. P., Ciais, P., Wieder, W. R., Abramoff, R., Huang, Y., Guenet, B., Prescher, A. K., Viscarra Rossel, R. A., Barre, P., Chenu, C., Zhou, G., & Tang, X.: Microbial dynamics and soil physicochemical properties explain large-scale variations in soil organic carbon, *Glob Chang Biol*, doi:10.1111/gcb.14994, 2020.

Zhou, M., Zhu, B., Wang, S., Zhu, X., Vereecken, H., & Bruggemann, N.: Stimulation of N_2O emission by manure application to agricultural soils may largely offset carbon benefits: a global meta-analysis, *Glob Chang Biol, 23*, 4068-4083, doi:10.1111/gcb.13648, 2017.